RSC Advances

RSC Publishing

PAPER

View Article Online
View Journal | View Issue

Cite this: *RSC Adv.*, 2013, **3**, 26017

Polypropylene/Mg_3Al–tartrazine LDH nanocomposites with enhanced thermal stability, UV absorption, and rheological properties

Qiang Wang,*[a] Jingwen Wu,[a] Yanshan Gao,[a] Zhang Zhang,[a] Junya Wang,[a] Xi Zhang,[b] Xingru Yan,[b] Ahmad Umar,[cd] Zhanhu Guo[b] and Dermot O'Hare*[e]

Received 18th August 2013
Accepted 10th October 2013

DOI: 10.1039/c3ra44452j

www.rsc.org/advances

We report the synthesis of coloured polypropylene (PP)/Mg_3Al–tartrazine layered double hydroxide (LDH) nanocomposites with enhanced thermal stability, UV absorption capacity, and rheological properties using a modified solvent mixing method for the first time. SEM images indicated that the LDH nanoparticles were evenly dispersed within the PP matrix due to the favourable interactions between PP and LDHs. TGA and DSC analysis indicated that the thermal stability of PP/LDH nanocomposites was significantly increased. Decreased G' and G'' ascribed to the enhanced mobility (relaxation) of the confined polymer chains at the interface of the PP/LDH layers suggested that the LDH is nano-dispersed in the composites. UV-Vis spectroscopy showed that the addition of Mg_3Al–tartrazine LDH significantly enhanced the UV absorption characteristics of PP. Since tartrazine is a nontoxic additive, these coloured PP/Mg_3Al–tartrazine LDH nanocomposites are expected to have many promising applications such as for food packing and children's toys, *etc.*

1. Introduction

Polypropylene (PP) has been utilised in a wide variety of fields including clothing, electronics, medical and chemical industry due to its high flexibility, good insulation and low cost. However, it has poor photostability and thermal stability. The UV component in sunlight can induce photo-oxidative degradation of PP, which has an adverse effect on its properties.[1,2] The polymer can also be oxidised at high temperature, a common problem during molding operations. To improve the UV resistance and thermal stability of PP, a cocktail of photostabilisers and anti-oxidants must be added to the PP during polymer processing.

Layered double hydroxides (LDHs) are a large class of ionic clays composed of positively charged brucite-like layers with an interlayer containing negatively charged compensating anions. The general formula can be represented as $[M_{1-x}^{2+}M_x^{3+}(OH)_2][A^{n-}]_{x/n}\cdot zH_2O$, where M^{2+} symbolises divalent metal cations, such as Mg^{2+}, Zn^{2+} or Ni^{2+} while M^{3+} embodies trivalent metal cations, *e.g.* Al^{3+}, Fe^{3+} or Mn^{3+}. A^{n-} indicates interlayer anions such as Cl^-, NO_3^-, CO_3^{2-}, RCO_2^-, and x is generally 0.2–0.4. z is the number of water molecules situated at the interlayer galleries together with the anions.[3,4] Significant effort has been devoted to finding different methods of synthesis of LDH materials due to their unique layered structure and anion exchangeability. LDHs have been used in various applications such as catalysts,[5] adsorbents,[6–9] ion exchange hosts,[10] and polymer additives.[11]

Several UV absorbers have been intercalated into LDHs.[12–16] It is found that the thermal stability of these guest chromophores within the interlayer space of LDHs have been markedly improved, which overall leads to the enhancement of both the photostability and thermal stability of these UV absorbers. PP containing intercalated materials has been shown to exhibit impressive UV photostability.[15–17]

Tartrazine also known as FD&C Yellow 5, or E102 in Europe, is an orange monoazo dye.[18] It has been widely used as additives in foods, pharmaceutical drugs, and cosmetics, *etc.* Tartrazine is an excellent UV absorber but exhibits poor thermal stability, which can be oxidised in the process of preparing polymer composites, restricting its use as a potential photostabiliser in polymers. The molecule structure of tartrazine is shown in Fig. 1(a). To date, several examples of tartrazine intercalated LDHs have been reported in the literature.[19,20] The tartrazine molecules are thought to interact with the positively charged host layers *via* their SO_3^- groups. The UV-Vis band of the intercalated dye is broadened by these interactions.

[a]*College of Environmental Science and Engineering, Beijing Forestry University, 35 Qinghua East Road, Haidian District, Beijing 100083, P. R. China. E-mail: qiang.wang.ox@gmail.com; qiangwang@bjfu.edu.cn; Tel: +86 13699130626*

[b]*Integrated Composites Laboratory, Dan F Smith Department of Chemical Engineering, Lamar University, Beaumont, TX 77710, USA*

[c]*Department of Chemistry, College of Science and Arts, Najran University, P.O. Box 1988, Najran-11001, Kingdom of Saudi Arabia*

[d]*Promising Centre for Sensors and Electronic Devices (PCSED), Najran University, P.O. Box 1988, Najran-11001, Kingdom of Saudi Arabia*

[e]*Chemistry Research Laboratory, Department of Chemistry, University of Oxford, 12 Mansfield Road, Oxford, OX1 3TA, UK. E-mail: dermot.ohare@chem.ox.ac.uk; Tel: +44 (0)1865 272686*

Fig. 1 (a) Molecular structure of tartrazine. (b) The schematic representation of the structure of Mg_3Al–tartrazine LDH and the picture of the LDH powder.

It is widely accepted that adding LDH nanofillers can significantly increase the thermal stability and tune the rheological property of polymers. However, up to date, the tartrazine intercalated LDHs have not been previously added into PP as nanofiller. We are very much interested to see if we could prepare high quality colorful PP/LDH–tartrazine nanocomposites with enhanced photo- and thermo-stability and rheological properties. In this contribution, PP/Mg_3Al–tartrazine nanocomposites were synthesised using a solvent mixing method for the first time. The synthesised Mg_3Al–tartrazine LDH and the corresponding PP/Mg_3Al–tartrazine LDH nanocomposites were systematically characterized. The properties of synthesised nanocomposites including thermal stability, UV absorption, and rheological property have been evaluated in detail.

2. Experimental

2.1 Synthesis

Mg_3Al–tartrazine LDH was synthesised using an anion exchange method. First, Mg_3Al–NO_3 was synthesised by a coprecipitation. A metal precursor solution containing 9.6 g $Mg(NO_3)_2 \cdot 6H_2O$ and 4.7 g $Al(NO_3)_3 \cdot 9H_2O$ in 50 ml H_2O was added drop-wise into the anion solution containing 2.125 g $NaNO_3$ in 50 ml H_2O, in the meantime, the pH was kept constant at 10 using NaOH (4 M). The mixture was aged at room temperature for 12 h, followed by filtration and washing with water until pH close to 7. The obtained water washed "wet cake" was directly used for the synthesis of Mg_3Al–tartrazine *via* anion exchange method. The above obtained Mg_3Al–NO_3 LDH "wet cake" was re-dispersed in 130 ml aqueous solution containing 20.04 g tartrazine. The pH of the solution was adjusted to 10 using NaOH (4 M), followed by aging at 70 °C for 12 h. After aging, LDH were separated by filtration and washed firstly with H_2O, then with acetone. After washing, the obtained LDH slurry was directly used for the preparation of PP/LDH nanocomposites.

PP/LDH nanocomposites were synthesised using a solvent mixing method. 5 g PP, the acetone washed Mg_3Al–tartrazine LDH slurry prepared above, and 100 ml xylene were loaded into a 250 ml round bottom flask. The amount of Mg_3Al–tartrazine LDH slurry added to the PP was adjusted to give LDH loadings of 0.4, 0.8, 1, 3, 6, 9 wt%, respectively. The mixture was refluxed at approximately 140 °C for 2 h. After the reflux process was finished, the hot xylene solution containing dissolved PP and the highly dispersed LDH nanoparticles was poured into 100 ml hexane (also called a solvent extraction method) in order to precipitate the PP/Mg_3Al–tartrazine LDH nanocomposite. The PP/Mg_3Al–tartrazine LDH nanocomposites were isolated by filtration and dried in vacuum at 65 °C.

2.2 Characterisation

XRD patterns were recorded on a PANalytical X'Pert Pro instrument in reflection mode with Cu Ka radiation. The accelerating voltage was set at 40 kV with 40 mA current (λ = 1.542 Å) at 0.01° s^{-1} from 1° to 70° with a slit size of 1/4 degree. FT-IR spectra were recorded on a Bio-Rad FTS 6000 FTIR Spectrometer equipped with a DuraSamplIR II diamond accessory in attenuated total reflectance (ATR) mode in the range of 400–4000 cm^{-1}; 100 scans at 4 cm^{-1} resolution were collected. The strong absorption in the range 2500–1667 cm^{-1} was from the DuraSamplIR II diamond surface. TEM analysis was performed on JEOL 2100 microscope with an accelerating voltage of 400 kV. Samples were dispersed in ethanol with sonication and then cast onto copper TEM grids coated with lacey carbon film. SEM and SEM-EDX analyses were performed on a JEOL JSM 6100 scanning microscope with an accelerating voltage of 20 kV. Powder samples were spread on carbon tape adhered to an SEM stage. Before observation, the samples were sputter coated with a thin platinum layer to prevent charging and to improve the image quality.

2.3 Polymer performance measurements

The thermal stability of neat PP and its LDH nanocomposites was studied by TGA (Netzsch), which was carried out with a heating rate of 10 °C min^{-1} in an air flow rate of 50 ml min^{-1} from 25 to 600 °C. The melt rheological behavior of neat PP and PP/Mg_3Al–tartrazine nanocomposites was studied using TA Instruments AR 2000ex Rheometer. An environmental test chamber (ETC) steel parallel-plate geometry (25 mm in diameter) was used to perform the measurement at 200 °C, with dynamic oscillation frequency sweeping from 100 to 0.1 Hz in the linear viscoelastic (LVE) range (strain 1%) under a nitrogen atmosphere to prevent the oxidation of PP. UV-Visible diffuse reflectance spectra were performed on a Lambda 750S UV-Vis spectrometer. The samples were first compressed into thin pellets before testing. The recrystallisation and melting behaviors of neat PP and nanocomposites were analysed by a TA Instrument Q200 differential scanning calorimeter (DSC). Experiments were run on samples of about 10 mg. Each sample was first heated from room temperature to 220 °C with a heating

rate of 10 °C min^{-1} to remove the thermal history, cooled to 40 °C at a rate of 10 °C min^{-1}, and then reheated to 220 °C at a rate of 10 °C min^{-1} to determine the melt temperature. The experiments were carried out at a nitrogen flow rate of 50 ml min^{-1}.

3. Results and discussion

3.1 Characterization of Mg_3Al–tartrazine LDH

The XRD patterns of Mg_3Al–NO_3 LDH and Mg_3Al–tartrazine LDH are shown in Fig. 2. The XRD pattern of Mg_3Al–NO_3 LDH precursor exhibits the typical characteristics of an LDH phase (Fig. 2(a)). Broad Bragg reflections indexed as (003), (006) and (009) are observed at $2\theta = 10.51°$, 21.45°, and 34.54°, respectively. The interlayer distance $d_{(003)}$ is calculated as 0.840 nm, which is very close to the reported value of 0.841 nm.[21] After the ion-exchange intercalation of tartrazine into the interlayer galleries of Mg_3Al–NO_3 LDH, the (003) and (006) Bragg reflections move to 3.84° and 8.04°, respectively (Fig. 2(b)). The corresponding interlayer separation $d_{(003)}$ is evaluated to be 2.30 nm, indicating the successful intercalation of tartrazine into Mg_3Al–NO_3 LDH to form Mg_3Al–tartrazine LDH. The (110) Bragg reflection located at 60.82°, which can be used to determine the *a*- and *b*-lattice parameters, remains almost unchanged after intercalation of tartrazine. There is a significant expansion in the structure perpendicular to the layers. The value of *c*-lattice parameter increases from 2.52 to 6.90 nm. Considering that one molecule of tartrazine has an approximate end-to-end length of 2.06 nm,[19] and that average thickness of one LDH layer is 0.46 nm,[22] it suggests that the tartrazine anions are tilted with an angle of *ca.* 66° with respect to the metal hydroxide layers. Fig. 1(b) shows the schematic structure of Mg_3Al–tartrazine LDH. The remaining of the reflection peak at 10.34° suggests that the nitrate anions should not be completely replaced by tartrazine. The thickness of the LDH nanoplates was calculated using Scherrer's equation. For Mg_3Al–NO_3, the thickness is around 3.4 nm, corresponding to about 4 brucite-like sheets. As we expected that after the intercalation of tartrazine, the thickness of the LDH nanoplates was enlarged to be around 6.3 nm. This data also suggested that the anion exchange was not 100% complete.

Fig. 3 shows the TGA analysis data of pure tartrazine, Mg_3Al–NO_3 LDH, and Mg_3Al–tartrazine LDH. For pure tartrazine, it showed four stage weight losses, with the first weight loss ends at around 200 °C. Considering the fact that most polymer processing requires a temperature as high as 180 °C, tartrazine molecules itself is not stable during these procedures. However, after being intercalated into the LDH gallery, its thermal stability was improved. It is clear that both Mg_3Al–NO_3 and Mg_3Al–tartrazine LDHs show the typical two stage weight losses. The first stage can be attributed to the loss of interlayer water. Up to *ca.* 180 °C, the weight losses for both Mg_3Al–NO_3 and Mg_3Al–tartrazine LDHs were exactly same, suggesting that the tartrazine did not decompose during this stage. The second weight loss between 200 and 500 °C should be attributed to the decomposition of interlayer anions and the partial dehydroxylation of the brucite-like layers.[23] In this stage, tartrazine must start to decompose since Mg_3Al–tartrazine LDH showed a much more weight loss than Mg_3Al–NO_3.

Fig. 4 shows the FTIR spectra of Mg_3Al–NO_3 LDH, pure tartrazine and Mg_3Al–tartrazine LDH. In the spectrum of Mg_3Al–NO_3 LDH, the strong absorption band at around 1382 cm^{-1} can be assigned to the intercalated nitrate.[24] The spectrum of tartrazine exhibits several distinctive absorptions, for instance we see absorbances at 1596 cm^{-1} from OH, 1552 cm^{-1} from C–C=N and C=C–N, 1478 cm^{-1} from C–N=N, 1414 cm^{-1} from N=N, 1345 cm^{-1} from C–N=N–C, 1178 cm^{-1} from C–N, and 1124, 1029, 1005, and 880 cm^{-1} from C–H vibrations.[25,26] The FTIR spectrum of Mg_3Al–tartrazine LDH (Fig. 4(b)) shows a very weak absorption band of the nitrate group, suggesting that most of the nitrate anions have been replaced by tartrazine anions, while characteristic absorbance bands due to tartrazine ions further confirms its intercalation.[27]

The morphology of synthesised Mg_3Al–tartrazine LDH was characterised by SEM and TEM analyses. The TEM image in Fig. 5(a) clearly shows the LDH nanoplatelets overlapping with each other. Fig. 5(b) represents the SEM image of the as-synthesised Mg_3Al–tartrazine LDH. Significant aggregation of the LDHs particles results upon dying, leading to big particles,

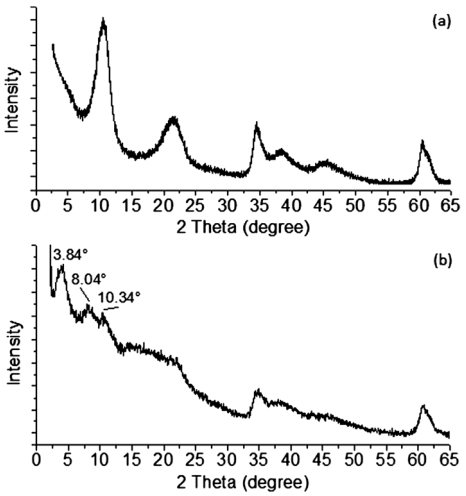

Fig. 2 XRD patterns for (a) Mg_3Al–NO_3 LDH and (b) Mg_3Al–tartrazine LDH.

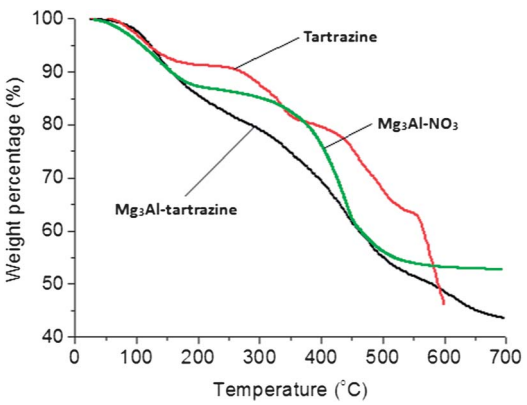

Fig. 3 TGA analysis of pure tartrazine, Mg_3Al–NO_3 LDH, and Mg_3Al–tartrazine LDH.

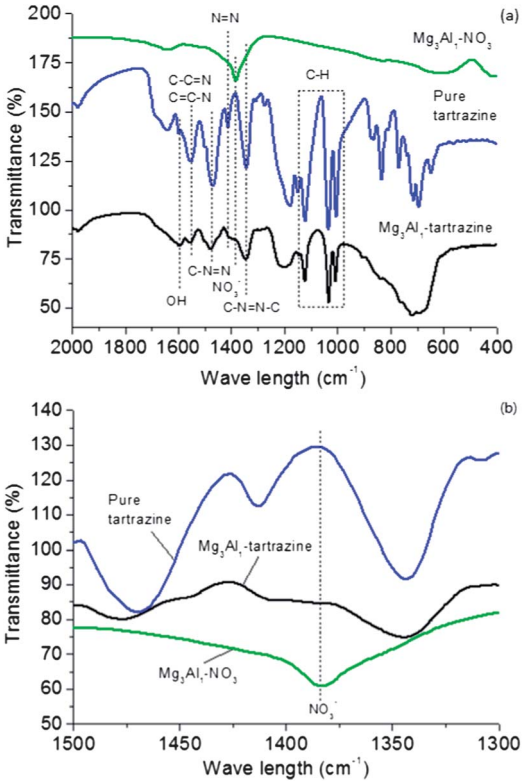

Fig. 4 FTIR analysis of Mg_3Al–NO_3 LDH, pure tartrazine and Mg_3Al–tartrazine LDH, (a) in the range of 2000–400 cm^{-1}, and (b) in the range of 1500–1300 cm^{-1}.

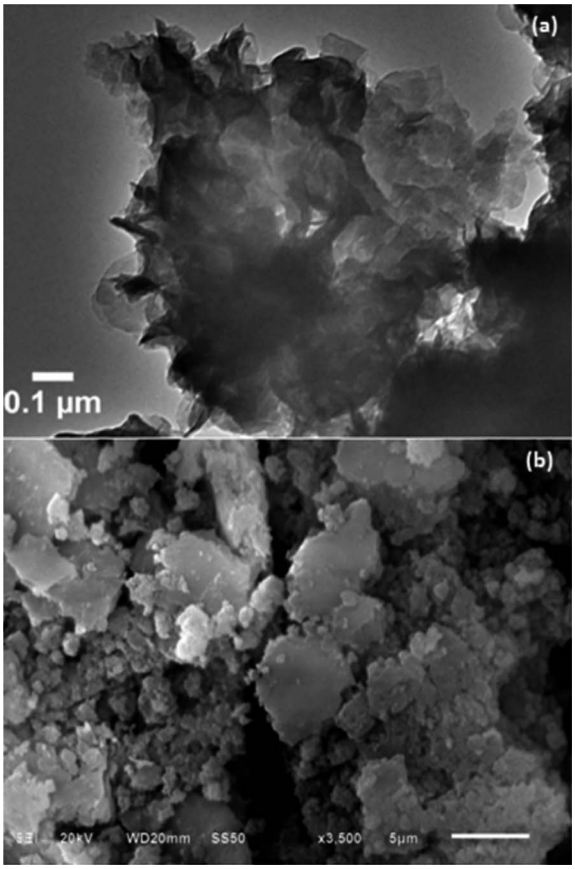

Fig. 5 (a) TEM and (b) SEM images of Mg_3Al–tartrazine LDH.

ranging from several to several-tenth micrometers. It is compelling evidence that LDH nanosheets should be introduced into polymer before the drying step. In our study, the PP/Mg_3Al–tartrazine LDH nanocomposite was prepared by a solvent mixing method, where xylene was used as the solvent. The LDH are first separated by filtration and washed initially with H_2O, then with acetone. After washing, the obtained LDH nanosheet slurry was directly dispersed in xylene. Due to the intercalation with tartrazine and the intensive acetone washing treatment, the LDH nanosheets behave as hydrophobic particles, leading to its highly dispersing in xylene.[28] PP/LDH composites was then prepared by dissolving PP in the LDH/xylene suspension at 140 °C for 2 h, followed by rapid precipitation by pouring the mixture into hexane.[29]

3.2 Characterisation of PP/LDH nanocomposites

The XRD data for the PP/LDH nanocomposites are shown in Fig. 6. The PP/LDH nanocomposites exhibit several characteristic reflections of Mg_3Al–tartrazine LDH. The intensity of these reflections increases with the increase in LDH loading. Wang *et al.*[29] observed that with dodecyl sulfate (DDS) intercalated Mg_3Al LDH, the gallery were expanded by the insertion of polymer molecules when the LDH loading is not high (0–2 wt%). However, in this study, we did not find any expansion of the Mg_3Al–tartrazine LDH gallery, and the interlayer separation remained the same at all LDH loadings (0–9 wt%).

PP/Mg_3Al–tartrazine LDH nanocomposites were also characterised using FT-IR analysis (Fig. 7). After introducing the LDHs, several characteristic absorbances due to the Mg_3Al–tartrazine LDH were observed. For instance, the absorbances at 1596 cm^{-1} and 1551 cm^{-1} can be attributed to OH, C–C=N and (C=C–N) vibrations respectively. The absorbances at 1124 cm^{-1} and 1032 cm^{-1} result form C–H vibrations.[25,26] The Al–O and Mg–O vibrations in the brucite-like layers were found at around 677 cm^{-1}, which agrees well with the literature.[8,30,31] When the

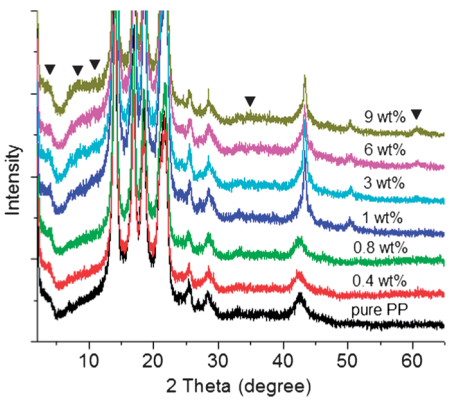

Fig. 6 XRD patterns of PP/Mg_3Al–tartrazine nanocomposites with LDH loadings of 0.4, 0.8, 1, 3, 6, 9 wt%. (▼) Mg_3Al–tartrazine LDH.

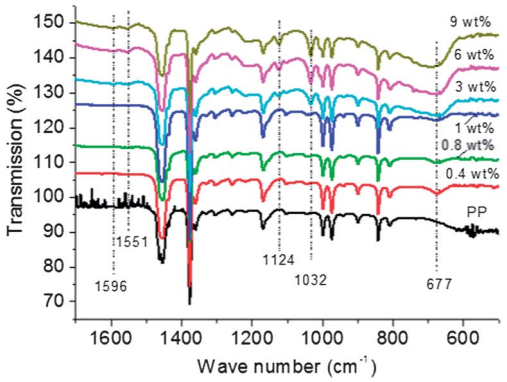

Fig. 7 FTIR analyses of pure PP and the PP/Mg_3Al–tartrazine nanocomposites with different LDH loadings (0.4, 0.8, 1, 3, 6, and 9 wt%).

LDH loading is low (no more than 1 wt%), the above mentioned characteristic peaks were very weak.

In order to study the morphology of obtained PP/Mg_3Al–tartrazine nanocomposites, SEM analysis was performed. Fig. 8 shows the SEM images of PP/Mg_3Al–tartrazine nanocomposites with various LDH loadings of 0.4, 0.8, 1, 3, 6 and 9 wt%. Because of the rapid precipitation of the polymer composite from hexane, spherical particles were formed for all the nanocomposites. We seldom observe any aggregated LDH particles when the loading is low (0.4–1 wt%), from which we can infer that there is a good dispersion of LDH particles within the PP matrix. The SEM image with a higher magnification in Fig. 8(g) clearly indicates that the surface of the nanocomposites is very clean and no LDH particles can be seen. In other words, the LDH nanoparticles should be mostly distributed within the PP matrix thanks to the solvent mixing method used in this contribution. However, with the increase of LDH loading from 3 to 9 wt%, the smoothness of the nanocomposite surface declines and more LDH nanoparticles can be clearly seen.

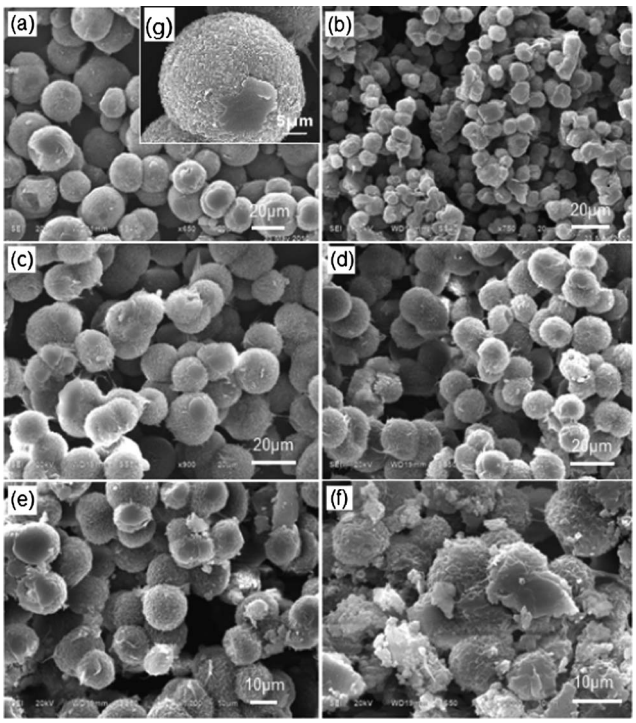

Fig. 8 SEM images of (a) 0.4 wt%, (b) 0.8 wt%, (c) 1 wt%, (d) 3 wt%, (e) 6 wt% and (f) 9 wt% PP/Mg_3Al–tartrazine nanocomposites. The inset of image (a) which is marked as (g) is the SEM images of 0.4 wt% PP/Mg_3Al–tartrazine nanocomposite with a higher magnification.

3.3 Properties of PP/Mg_3Al–tartrazine LDH nanocomposites

The thermal stability of PP/Mg_3Al–tartrazine LDH nanocomposites with different loadings was tested using TGA (Fig. 9). The 10% weight loss temperature ($T_{0.1}$) data and 50% weight loss temperature ($T_{0.5}$) data clearly indicate that the thermal stability of Mg_3Al–tartrazine LDH loaded PP nanocomposites is significantly enhanced comparing to pure PP. Surprisingly we found that with only 0.4–0.8 wt% of LDH, the $T_{0.1}$ and $T_{0.5}$ were increased by 26.2 and 41.3 °C, respectively. This is very rare as many inorganic nanoparticle filled nanocomposites that need around 10 wt% loading to achieve its highest $T_{0.5}$ increase.[28,32,33] However, Wang *et al.*[29] found that when the LDH is intercalated with DDS, the highest $T_{0.5}$ increase for PP/LDH nanocomposites was also observed in low LDH loading range (1 wt%). This probably stems from the strengthened interaction between PP and LDHs by the hydrophobic tail of intercalated anions. Further increase in LDH loading from 0.8 wt% up to 6 wt% only resulted in a slight decrease in $T_{0.1}$ and $T_{0.5}$. However, if the LDH loading is up to 9 wt%, the thermal stability of the nanocomposite became much worse. The $T_{0.5}$ was only increased by 12.2° while the $T_{0.1}$ was decreased by 11.3°. Therefore, it can be concluded from the TGA data that in order to have the optimum thermal stability then Mg_3Al–tartrazine LDH loading should be not be higher than 6 wt%.

The melting and recrystallisation characteristics of both the PP and PP/LDH nanocomposites are significant parameters when considering the downstream processing of these materials. Table 1 describes melting and recrystallisation events. In this work, the DSC curves were recorded during the first and second heating processes. Both the melting temperature (T_m)

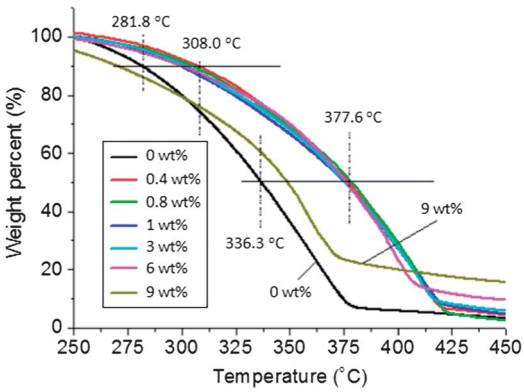

Fig. 9 Thermal stability of PP/Mg_3Al–tartrazine LDH nanocomposites evaluated by TGA.

and the recrystallisation temperature (T_c) increased after introducing LDHs. With 1 wt% loading, T_c and T_m increased by 6.77 °C and 2.55 °C, respectively. As the LDH loadings gradually rose, the difference in both T_c and T_m declined. The crystallinity fraction (X_c) of pure PP and PP/LDH nanocomposites was determined by eqn (1), where the crystallinity heat of pure PP (ΔH_c^0) was assumed to be 146.5 J g^{-1}.[34,35] At 1 wt% and 3 wt% loadings, the nanocomposites exhibit a huge enhancement of X_c by *ca.* 9.8% and 6.7% compared to pure PP, respectively. When the loading is at 6 wt%, the X_c drops to 57.5%, which is 0.7% less than pure PP. At 9 wt% loading, the X_c continues to decrease by 4.4% compared to pure PP.

$$X_c = \frac{\Delta H_c}{\Delta H_c^o} \times 100 \quad (1)$$

The rheological behavior of the nanocomposite melt is an essential for the industrial processing of these materials. The formation of a percolated system can be detected by identifying the complex viscosity (η^*), storage modulus (G') and loss modulus (G'') as a function of frequency (w).[36–38] The storage and loss moduli of pure PP and its nanocomposites melts containing the nanoplatelet LDHs from 1 to 9 wt% at 200 °C are outlined in Fig. 10. These PP/LDH nanocomposites exhibited decreased G' and G'', which can be ascribed to the enhanced mobility (relaxation) of confined polymer chains at the interface of PP/LDH layers.[39,40] Such relaxation behavior supports the conclusion that the LDH is nano-dispersed in the composite.[41,42] The complex viscosity $\eta^*(w)$ has a strong relationship with G' and G'' and can be calculated by eqn (2). Thus the reduced viscosity can be outlined in Fig. 10. G' and G'' first decreased with increasing LDH loading to 6 wt% and then began to rise with further increasing LDH loading to 9 wt%.

$$\eta^*(\omega) = \left[(G'/\omega)^2 + (G''/\omega)^2\right]^{1/2} \quad (2)$$

Fig. 11(a) shows the η^* as a function of w for pure PP and its nanocomposites at 200 °C. η^* firstly decreased with increasing LDH loading up to 6 wt% and then began to increase with the further increase of LDH loading up to 9 wt%. The pure PP describes a typical viscoelastic behavior characterised by a transition from low frequency Newtonian flow behavior to high frequency shear thinning nature.[43–45] Such fluid properties were also observed in the PP/LDH nanocomposites with the LDH loading of 9 wt%. The introducing of fillers causes the complex viscosity decrease, the reduced viscosity may result from

Table 1 Summary of the melting temperature (T_m), ΔH_c and the recrystallisation temperature (T_c), ΔH_m and crystallinity fraction (X_c) as measured by DSC for the PP/Mg–Al–tartrazine nanocomposites

LDH loading (wt%)	T_c (°C)	ΔH_c (J g^{-1})	T_m (°C)	ΔH_m (J g^{-1})	X_c (%)
0	108.31	85.61	153.65	85.70	58.4
1	115.08	99.92	156.20	95.89	68.2
3	117.34	95.44	152.19	89.04	65.1
6	118.51	84.29	156.50	79.39	57.5
9	119.01	79.12	156.73	75.21	54.0

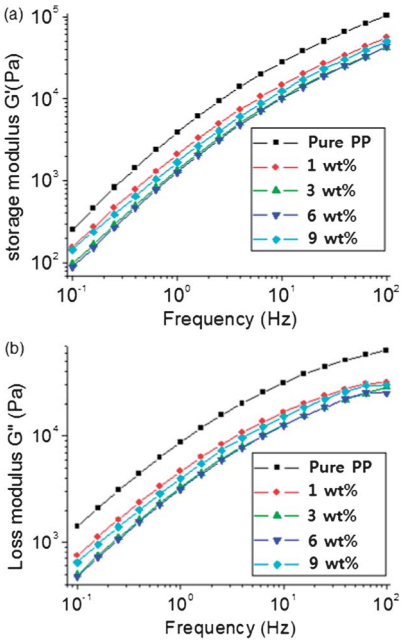

Fig. 10 (a) Storage modulus (G') and (b) loss modulus (G'') as a function of frequency for PP and PP/LDH nanocomposites.

increment of free volume, dilution effect and constraint release of matrix polymer. In some systems, when the average nanoparticle separation distance is smaller than twice the polymer radius of gyration R_g, the nanoparticles will perturb polymer chain configurations and lead to reduced viscosity. G' *versus* G'' for neat PP and its nanocomposites is plotted in Fig. 11(b). A nearly linear relationship between G' and G'' was observed for all samples, particularly at low ω regime, and G' increases with the increase of G''. After introducing LDHs, the ratio of G'/G''

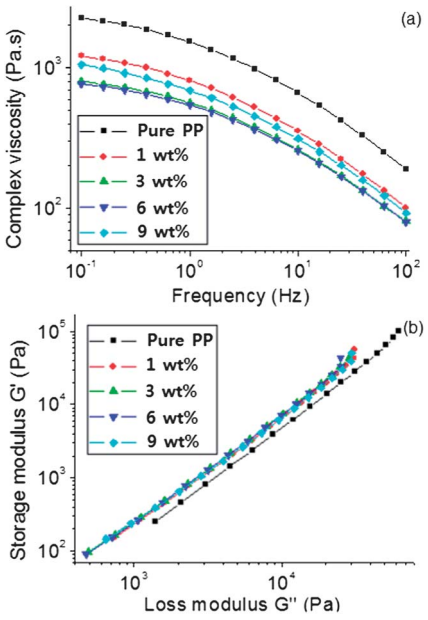

Fig. 11 (a) The complex viscosity as a function of frequency for the pure PP and PP/LDH nanocomposites, and (b) the storage *vs.* loss modulus.

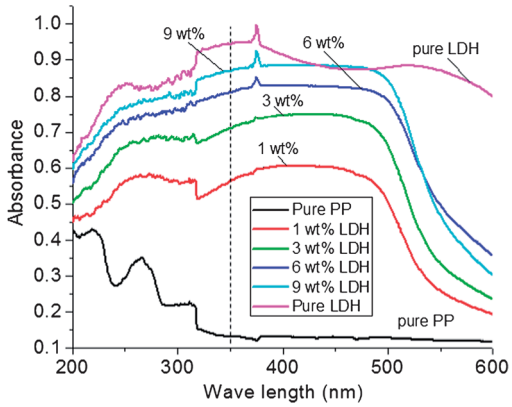

Fig. 12 UV-Visible absorption of PP/Mg_3Al–tartrazine nanocomposites.

was increased in the whole ω range, with the slope remaining the same. This data suggests that the structure of nanocomposites across the length scales did not change on increasing the LDH loading.[43,46,47]

As it's well known that tartrazine has a good UV absorption ability, thus the UV absorption of pure PP, pure Mg_3Al–tartrazine LDH, and PP/Mg_3Al–tartrazine LDH nanocomposites was measured, as shown in Fig. 12. The data for pure Mg_3Al–tartrazine LDH shows strong UV absorption between 300 and 480 nm, which results from the presence of tartrazine anions in the interlayer galleries. The curve of pure PP indicates that it has very poor UV absorption capacity, particularly in the range of 300–400 nm. However, introducing Mg_3Al–tartrazine LDH significantly enhanced its UV absorption characteristics. The UV absorption capacity showed an upward trend with the increase in LDH loading. For instance, at 350 nm, the UV absorbance increased from 14% for pure PP to 59% for 1 wt% loading. The absorbance further increased to 75%, 85%, and 92% for 3 wt%, 6 wt% and 9 wt%, respectively. This result confirms that the UV absorption capacity of PP can be significantly enhanced by the introduction of Mg_3Al–tartrazine LDH.

4. Conclusions

In this contribution, we have successfully prepared highly dispersed PP/Mg_3Al–tartrazine LDH nanocomposites containing different LDH loadings from 0.4–9 wt% using a modified solvent mixing method. The orange Mg_3Al–tartrazine LDH nanoadditive imparts good colour stability to the polymer. When the LDH loading is low (no more than 1 wt%), the LDH nanoparticles had a good dispersion within PP matrix. SEM images showed that spherical particles were formed for all the nanocomposites. No aggregated LDH particles can be observed when the loading is low (0.4–1 wt%). Due to the good interaction between PP and LDHs, the thermal stability of PP/LDH nanocomposites was significantly increased. With only 0.4–0.8 wt% of Mg_3Al–tartrazine LDH, the $T_{0.1}$ and $T_{0.5}$ were increased by 26.2 and 41.3 °C, respectively. DSC analysis demonstrated that both T_m and T_c were increased by adding Mg_3Al–tartrazine LDH. Rheological analysis suggested that these PP nanocomposites filled with Mg_3Al–tartrazine LDHs exhibited decreased G', G'', and η^*. UV analysis proved that introducing Mg_3Al–tartrazine LDH can significantly enhance the UV absorption ability of PP. The UV absorbance increased from 14% for pure PP to 59%, 75%, 85%, and 92% for 1 wt%, 3 wt%, 6 wt% and 9 wt%, respectively. In all, we have demonstrated that the thermal stability, melt and recrystallisation behavior, rheological property, and UV absorption can be enhanced by adding only small amount of Mg_3Al–tartrazine LDH.

Acknowledgements

The authors thank the Fundamental Research Funds for the Central Universities (TD-JC-2013-3), the Program for New Century Excellent Talents in University (NCET-12-0787), the Beijing Nova Programme (Z131109000413013), the National Natural Science Foundation of China (51308045), the Key Laboratory of Functional Inorganic Material Chemistry (Heilongjiang University), Ministry of Education, and the SCG Chemicals, Thailand for financial support.

References

1 S. Sasakia, S. Aisawaa, H. Hiraharaa, A. Sasakib, H. Nakayamac and E. Naritaa, *J. Solid State Chem.*, 2006, **179**, 1129.
2 J. Zhao, X. Yin, J. Shi, X. Zhao, X. Wang, M. Chen, Z.-M. Dang and G.-H. Hu, *Sci. Adv. Mater.*, 2013, **5**, 505.
3 Q. Wang and D. O'Hare, *Chem. Rev.*, 2012, **112**, 4124.
4 Q. Wang, Y. Gao, Z. Zhang, L. Duan, A. Umar and D. O'Hare, *Sci. Adv. Mater.*, 2013, **5**, 411.
5 X. Xu, R. Lu, X. Zhao, S. Xu, X. Lei, F. Zhang and D. G. Evans, *Appl. Catal., B*, 2011, **102**, 147.
6 Q. Wang, J. Luo, Z. Zhong and A. Borgna, *Energy Environ. Sci.*, 2011, **4**, 42.
7 Q. Wang, H. H. Tay, D. J. W. Ng, L. Chen, Y. Liu, J. Chang, Z. Zhong, J. Luo and A. Borgna, *ChemSusChem*, 2010, **3**, 965.
8 Q. Wang, Z. Wu, H. H. Tay, L. Chen, Y. Liu, J. Chang, Z. Zhong, J. Luo and A. Borgna, *Catal. Today*, 2011, **164**, 198.
9 Q. Wang, J. Yu, J. Liu, Z. Guo, A. Umar and L. Sun, *Sci. Adv. Mater.*, 2013, **5**, 469.
10 F. Millange, R. I. Walton, L. Lei and D. O'Hare, *Chem. Mater.*, 2000, **12**, 1990.
11 F. Leroux and J. P. Besse, *Chem. Mater.*, 2001, **13**, 3507.
12 H. Chai, X. Xu, Y. Lin, D. G. Evans and D. Li, *Polym. Degrad. Stab.*, 2009, **94**, 744.
13 H. Chai, Y. Lin, D. G. Evans and D. Li, *Ind. Eng. Chem. Res.*, 2008, **47**, 2855.
14 G. Cui, D. G. Evans and D. Li, *Polym. Degrad. Stab.*, 2010, **95**, 2082.
15 L. Zhang, Y. Lin, Z. Tuo, D. G. Evans and D. Li, *J. Solid State Chem.*, 2007, **180**, 1230.
16 H. Zhu, Y. Feng, P. Tang, G. Cui, D. G. Evans, D. Li and X. Duan, *Ind. Eng. Chem. Res.*, 2011, **50**, 13299.
17 D. Li, Z. Tuo, D. G. Evans and X. Duan, *J. Solid State Chem.*, 2006, **179**, 3114.

18 N. Peica, I. Pavel, S. C. Pinzaru, V. K. Rastogi and W. Kiefer, *J. Raman Spectrosc.*, 2005, **36**, 657.
19 L. Benes, K. Melanova, V. Zima and J. Svoboda, *Collect. Czech. Chem. Commun.*, 2005, **70**, 259.
20 C. Taviot-Guehoa, A. Illaik, C. Vuillermoz, S. Commereuc, V. Verney and F. Leroux, *J. Phys. Chem. Solids*, 2007, **68**, 1140.
21 I. F. Alexa, R. F. Popovici, M. Ignat, E. Popovici and V. A. Voicu, *Digest.J. NanoMater. BioStruct.*, 2011, **6**, 1091.
22 B. J. Teppen, K. Rasmussen, P. M. Bertsch, D. M. Miller and L. Schäfer, *J. Phys. Chem. Solids*, 1997, **101**, 1579.
23 T. Vlase, G. Vlase, M. Modra and N. Doca, *J. Therm. Anal. Calorim.*, 2007, **88**, 389.
24 Z. P. Xu and H. C. Zeng, *Chem. Mater.*, 2001, **13**, 4564.
25 N. Peica, I. Pavel, S. Cinta Pinzaru, V. K. Rastogi and W. Kiefer, *J. Raman Spectrosc.*, 2005, **36**, 657.
26 http://www.hanhonggroup.com/ir/ir_en/RE04000046.html.
27 P. Tang, X. Xu, Y. Lin and D. Li, *J. Appl. Chem.*, 2008, **47**, 2478.
28 Q. Wang, X. Zhang, J. Zhu, Z. Guo and D. O'Hare, *Chem. Commun.*, 2012, **48**, 7450.
29 Q. Wang, X. Zhang, C. J. Wang, J. Zhu, Z. Guo and D. O'Hare, *J. Mater. Chem.*, 2012, 19113.
30 W. Kagunya, R. Baddour-Hadjean, F. Kooli and W. Jones, *Chem. Phys.*, 1998, **236**, 225.
31 Z. P. Xu and G. Q. Lu, *Chem. Mater.*, 2005, **17**, 1055.
32 X. Chen, S. Wei, A. Yadav, R. Patil, J. Zhu, R. Ximenes, L. Sun and Z. Guo, *Macromol. Mater. Eng.*, 2011, **296**, 434.
33 Y. Li, J. Zhu, S. Wei, J. Ryu, L. Sun and Z. Guo, *Macromol. Chem. Phys.*, 2011, **212**, 1951.
34 S. P. Lonkar, S. Morlat-Therias, N. Caperaa, F. Leroux, J. L. Gardette and R. P. Singh, *Polymer*, 2009, **50**, 1505.
35 M. Eder and A. Wlochowicz, *Polymer*, 1983, **24**, 1593.
36 J. Zhu, S. Wei, J. Ryu, M. Budhathoki, G. Liang and Z. Guo, *J. Mater. Chem.*, 2010, **20**, 4937.
37 J. Zhu, S. Wei, A. Yadav and Z. Guo, *Polymer*, 2010, **51**, 2643.
38 C. A. Mitchell, J. L. Bahr, S. Arepalli, J. M. Tour and R. Krishnamoorti, *Macromolecules*, 2002, **35**, 8825.
39 F. R. Costa, M. Saphiannikova, U. Wagenknecht and G. Heinrich, *Adv. Polym. Sci.*, 2008, **210**, 101.
40 G. Barut, P. Pissis, R. Pelster and G. Nimtz, *Phys. Rev. Lett.*, 1998, **80**, 3543.
41 A. Huwe, F. Kremer, P. Behrens and W. Schwieger, *Phys. Rev. Lett.*, 1999, **82**, 2338.
42 J. Baschnagel, C. Mischler and K. Binder, *J. Phys. IV*, 2000, **10**, Pr7-9–Pr7-14.
43 J. Zhu, S. Wei, Y. Li, L. Sun, N. Haldolaarachchige, D. P. Young, C. Southworth, A. Khasanov, Z. Luo and Z. Guo, *Macromolecules*, 2011, **44**, 4382.
44 A. J. Poslinski, M. E. Ryan and R. K. Gupta, *J. Rheol.*, 1988, **32**, 703.
45 A. V. Shenoy, *Rheology of filled polymer systems*, Kluwer Academic, Dordrecht, The Netherlands, 1999.
46 T. McNally, P. Potschke, P. Halley, M. Murphy, D. Martin, S. E. J. Bell, G. P. Brennan, D. Bein, P. Lemoine and J. P. Quinn, *Polymer*, 2005, **46**, 8222.
47 P. Potschke, M. Abdel-Goad, I. Alig, S. Dudkin and D. Lellinger, *Polymer*, 2004, **45**, 8863.